

## Proximity effect and boundary conditions in superconducting-normal double layers

H. J. Fink\* and M. Sheikholeslam\*

*Department of Electrical Engineering, University of California, Davis, California 95616*

A. Gilabert, J. P. Laheurte, J. P. Romagnan, and J. C. Noiray

*Laboratoire de Physique de la Matière Condensée, Université de Nice, Parc Valrose, 06034 Nice Cedex, France*

E. Guyon

*Laboratoire de Physique des Solides, Université de Paris-Sud, 91405 Orsay, France*

(Received 23 February 1976)

The nucleation fields for superconducting-normal ( $s$ - $n$ ) double layers are calculated for arbitrary thicknesses of the  $s$  and  $n$  layers when the applied magnetic field is parallel to the  $s$ - $n$  interface. One boundary condition was left undetermined in the calculation. Experiments were performed on Pb-Cu and Pb-Sn double layers for various thicknesses of the  $s$  and  $n$  layers. The boundary condition was extracted by comparing the theoretical and experimental results. It is found that the effective pair potential is approximately continuous across the  $s$ - $n$  boundary for a large range of temperatures and all thicknesses of the  $s$  and  $n$  layers. A simple model is proposed to explain this continuity in terms of an effectively induced pair potential in the  $n$  metal near the  $s$ - $n$  boundary which is controlled by an electron-phonon interaction different from that in the bulk of the  $n$  metal. The nucleation fields of the Pb-Sn double layers as a function of temperature are "S-shaped" when Pb is thin, whereas those of Pb-Cu are well behaved. It is proposed that the coherence (extrapolation) length of Sn is magnetic field dependent.

### I. INTRODUCTION

The largest magnetic field  $H_0$  up to which superconductivity exists in superconducting-normal ( $s$ - $n$ ) double layers has been studied both theoretically and experimentally for  $s$ - $n$  sandwiches of arbitrary thickness. The direction of  $H_0$  is parallel to the  $s$ - $n$  interface at which the proximity effect controls the amount of superconductivity.

The model of the proximity effect considered by the Orsay Group<sup>1</sup> and Deutscher<sup>2</sup> applies to the dirty limit<sup>3</sup> and does not include explicitly the thickness of the  $n$  layer. The proximity effect is taken into account by an extrapolation length<sup>4,5</sup>  $b$  of the pair potential of the  $s$  region into the  $n$  region at the  $s$ - $n$  interface.

In Refs. 6 and 7 a model was developed in which the extrapolation length  $b$  does not appear explicitly. The upper critical field  $H_0$  was calculated when both the  $n$  and  $s$  regions are thick<sup>6</sup> compared to the coherence lengths of the superconductor  $\xi$  and the normal metal  $|\xi_n|$ , and when the  $n$  region is very thick and the  $s$  region of finite thickness<sup>7</sup>  $d_s$ . Both calculations<sup>6,7</sup> are general and include both the dirty and the clean limits. The  $n$  metal may be a normal metal or a superconductor above its bulk transition temperature  $T_{cn}$ . One of the boundary conditions at the  $s$ - $n$  interface is left undetermined in the calculations and it can be related directly to Gor'kov's<sup>8</sup> microscopic theory and also to the measured critical field  $H_0$ . Thus by measuring the upper critical field one obtains information con-

cerning the boundary conditions at the  $s$ - $n$  interface.

There are a number of experimental results of the upper critical field  $H_0$  for  $s$ - $n$  systems.<sup>9-18</sup> The most recent experimental results on Pb-Ag and Pb-Cu sandwiches by Todd *et al.*<sup>17,18</sup> have been analyzed by the above model.<sup>6,7</sup> They show that the most satisfactory boundary condition which describes the experimental results is a boundary condition obtained by Zaitsev<sup>19</sup> for specular electron reflection at the  $s$ - $n$  interface, namely, the continuity of the pair potential  $\Delta_G$ . Similar conclusions were reached by Fink<sup>20</sup> when analyzing experimental results by Jain and Tilley<sup>21</sup> of Cu-Pb-Cu triple layers for thick Cu layers.

It is the purpose of this work to study both theoretically and experimentally the superconducting nucleation field  $H_0$  of  $s$ - $n$  double layers for arbitrary thicknesses of the normal and superconducting layers (generalization of the model of Refs. 6 and 7) over a wide range of temperatures when the applied magnetic field is applied parallel to the  $s$ - $n$  interface. The boundary conditions at the  $s$ - $n$  interface, which are of great theoretical and practical importance, are left adjustable in the theoretical part of this work. In the experimental part of this work, various theoretical boundary conditions are tested by the experimental results. One set of specimens consists of two superconductors with different transition temperatures  $T_{cn}$  and  $T_{cs}$ , the other of a superconductor and a normal metal (Cu). Preliminary results of the second set of materials were reported<sup>22</sup> recently.

## II. THEORETICAL MODEL

### A. Preamble

We consider a superconducting-normal double layer in a magnetic field  $H_0$  applied parallel to the  $s$ - $n$  interface (Fig. 1). The  $n$  layer is of thickness  $d_n$  and the  $s$  layer of thickness  $d_s$ . The other dimensions are assumed to be very large in comparison to  $d_n$  and  $d_s$ . The coordinate perpendicular to  $H_0$  is  $x$  or in the below normalization  $\zeta$ . The  $n$  metal is either a superconductor below its transition temperature  $T_{c_n}$ , which is lower than that of the  $s$  metal  $T_{c_s}$ , or it is a normal metal.  $\xi_n$  may be interpreted as an imaginary *bulk* coherence length for  $T > T_{c_n}$ .

Nucleation of superconductivity occurs by a second-order phase transitions at the largest magnetic field  $H_0$  (defined as the nucleation field) and is controlled by the free surface of the  $s$  layer. If  $d_s$  is very large in comparison to the *bulk* coherence length  $\xi(T)$  of the  $s$  metal, the proximity effect due to the  $n$  metal at the interface at  $x=0$  (see Fig. 1) will be of no consequence concerning the nucleation process near the free surface at  $x=d_s$ . The amount of superconductivity induced in or transferred to the  $n$  metal will have an insignificant effect on the nucleation process. However, if  $d_s$  is of order of magnitude of  $\xi(T)$ , the relative amount of superconductivity transferred to the  $n$  layer can become significant, in particular if  $d_n$  is small in comparison to  $\xi_n$ . On the other hand, if  $d_n$  is large and  $d_s$  is small, the proximity effect at  $x=0$  will act upon the superconducting nucleation process near the free surface in a detrimental way such that it may inhibit nucleation of superconductivity altogether. Furthermore, a decrease in the thickness  $d_s$  has the inherent tendency, as for a thin superconducting layer not in contact with a normal metal, to increase the nucleation field of that layer due to the favorable gain in the magnetic field energy as the thickness is reduced. Thus, we expect that a complicated interplay between the proximity effect, the nucleation processes and the size dependences of the  $s$  and  $n$  layers will determine the parallel nucleation field  $H_0$ .

We follow, in principle, a method similar to that used in calculating  $H_0$  for a  $n$ - $s$ - $n$  triple layer.<sup>20</sup>

### B. Eigenvalue equations and their solutions

Nucleation of superconductivity follows closely that of surface superconductivity. Therefore, we may assume that we are dealing with a second-order phase transition and may neglect the cubic term in the first Ginzburg-Landau equation. Assuming that the  $s$ - $n$  interface is at  $x=0$  (see Fig.

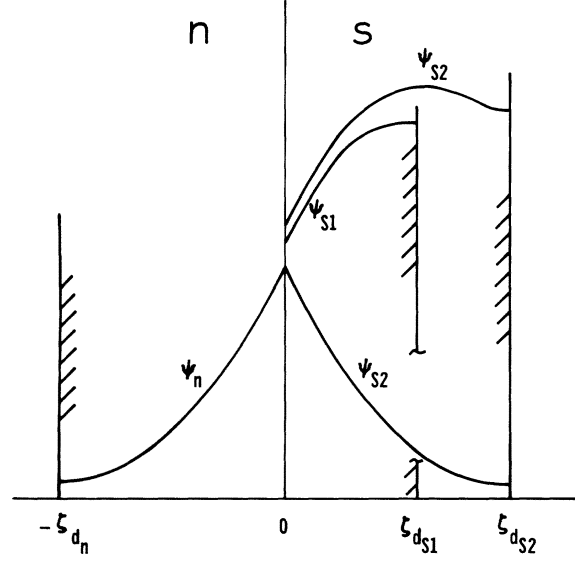


FIG. 1. Effect of the proximity effect on the order parameter is shown schematically for a  $s$ - $n$  double layer of thickness  $d_n + d_s$ .  $\psi_s$  has a maximum away from the free surface if  $d_s$  is large in comparison to  $\xi(T)$ . If  $d_s \lesssim \xi(T)$ , the maximum of  $\psi_s$  is at the free surface.  $\psi_n$  has always a minimum at the free surface if the  $n$  metal is in the normal state. Solutions of  $\psi_{s2}$  obtained from Eq. (1) are similar to those of  $\psi_n$  obtained from Eq. (2).

1), the appropriate equations for the amplitudes of the order parameters are<sup>6,7</sup>

$$-\frac{d^2\psi_s}{d\zeta^2} + (\zeta - \Gamma)^2\psi_s = \epsilon\psi_s \quad \text{for } 0^+ \leq \zeta \leq \zeta_{d_s}, \quad (1)$$

$$-\frac{d^2\psi_n}{d\zeta^2} + (\zeta - \Gamma_n)^2\psi_n = \epsilon_n\psi_n \quad \text{for } -\zeta_{d_n} \leq \zeta \leq 0^-. \quad (2)$$

We make the following assumptions and use the following definitions: For the order parameters we write  $\Psi_s(x, y) = \psi_s(x) \exp(-iky)$  and  $\Psi_n(x, y) = \psi_n(x) \exp(-ik_n y)$ . The coordinate perpendicular to the  $s$ - $n$  boundary is written in normalized dimensionless units as

$$\zeta = x(2\pi H_0/\phi_0)^{1/2}, \quad (3)$$

where  $\phi_0$  is the fluxoid quantum. The eigenvalues of Eqs. (1) and (2) are

$$\epsilon \equiv H_{c2}/H_0 = \phi_0/2\pi H_0 \xi^2 \quad (4)$$

and

$$\epsilon_n/\epsilon = \xi(T)^2/\xi_n(T)^2 \equiv \alpha(T). \quad (5)$$

We choose a gauge such that the vector potential is zero at  $x=0$ . The locations of the normalized nucleation centers measured from  $\zeta=0$  are  $\Gamma = (\phi_0/2\pi H_0)^{1/2}k$  and  $\Gamma_n = (\phi_0/2\pi H_0)^{1/2}k_n$ . The normalized slopes of the order parameters for the

$s$  and  $n$  layers are (see Fig. 1)

$$S = \left. \frac{d\psi_s(\zeta)/\psi_s(0^+)}{d\zeta} \right|_{0^+}, \quad (6)$$

$$S_n = \left. \frac{d\psi_n(\zeta)/\psi_n(0^-)}{d\zeta} \right|_{0^-}. \quad (7)$$

At the free surfaces the boundary conditions are

$$S = 0 \text{ at } \zeta = \zeta_{d_s}, \quad (8)$$

$$S_n = 0 \text{ at } \zeta = -\zeta_{d_n}, \quad (9)$$

and  $S$  and  $S_n$  are indetermined as yet at  $\zeta = 0^+$  and  $0^-$ , respectively.

The linear equation (1) was solved numerically by first selecting the values of the normalized thickness of the  $s$  layer,  $\zeta_{d_s}$ . A value of  $\Gamma$  was chosen,  $\psi_s(0^+)$  was made equal to unity, and the slope  $S$  at  $\zeta = 0^+$  was chosen a fixed value. Then the function  $\psi_s(\zeta)$  was generated and  $\epsilon$  was varied until boundary condition (8) was satisfied at  $\zeta_{d_s}$ . This was done for different values of  $\Gamma$  until  $\epsilon$  reached an absolute minimum while  $S$  was kept the same. The distance of the nucleation center in the  $s$  layer in conventional units,  $x_n$ , from the  $s$ - $n$  boundary is  $x_n/\xi = \Gamma\sqrt{\epsilon}$  and the renormalized thickness of the  $s$  layer is  $d_s/\xi = \zeta_{d_s}\sqrt{\epsilon}$ .

This minimum value of  $\epsilon$  ( $\equiv H_{c2}/H_0$ , largest nucleation field  $H_0$ ) is shown in Fig. 2 as a function of the square of the renormalized thickness of the  $s$  layer,  $(d_s/\xi)^2$ , for various values of the normalized slope of the order parameter  $S$  at  $\zeta = 0^+$  [Eq. (6)]. Since negative values of  $S$  may lead to negative values of  $\epsilon$ , this kind of plot includes also, implicitly, the general results for the  $n$  layer as is apparent from Fig. 1.

### C. Matching at boundary and the nucleation field of the $s$ - $n$ double layer

The appropriate boundary conditions at the  $s$ - $n$  interface,<sup>19</sup> assuming that the superconducting phase current density is continuous at the  $s$ - $n$  interface, are

$$S_n = \gamma S \quad (10)$$

and

$$\gamma = (m_n/m_s)\psi_s^2(0^+)/\psi_n^2(0^-). \quad (11)$$

$m_n$  and  $m_s$  are the effective electron masses on the  $n$  and  $s$  sides, respectively. The value of  $\gamma$  is indetermined at this point and will be determined by the experiments below.  $\gamma$  is a measure of the relative strengths of superconductivity at the boundary. Both parameters  $\alpha(T)$  and  $\gamma$  can be related to microscopic properties and are therefore of physical significance. We, therefore, express  $H_0$  as a function of  $\alpha(T)$  and  $\gamma$  for various thicknesses  $d_s$  and  $d_n$  of the  $s$  and  $n$  layers, respectively. This

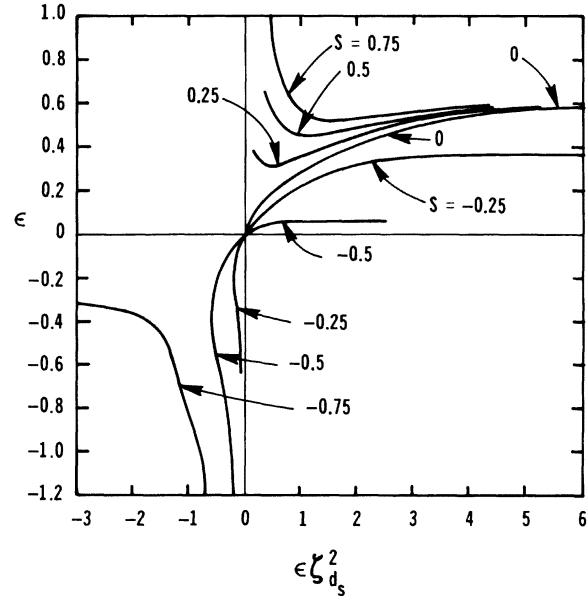


FIG. 2. Lowest eigenvalues of Eq. (1) as a function of the thickness  $d_s$  of the  $s$  layer for various boundary condition  $S$  as defined by Eq. (6). Note that  $\epsilon \zeta_{d_s}^2 = (d_s/\xi)^2$ .

was done the following way.

From an extensive plot like Fig. 2 curves of  $\epsilon$  vs  $S$  were constructed with  $d_s/\xi$  or  $d_n/\xi$  equal to a constant value. Note that in both cases  $\xi$  is the bulk coherence length of the  $s$  metal. For constant values of  $d_s/\xi$  and  $\gamma$  we choose an arbitrary value of  $S$ , determine from this  $S$  value the value of  $\epsilon \equiv H_{c2}/H_0$  from the above graph, and calculate  $S_n$  from Eq. (10). Since a negative value of  $S$  in Fig. 1 for the  $s$  layer solution has the same meaning as a positive value of  $S_n$  for the corresponding solution in the  $n$  layer, one may obtain from the above plot (Fig. 2) for a fixed value of  $S_n$  and a fixed value of  $d_n/\xi$  the corresponding  $\epsilon_n$  value which may be positive or negative. If  $\epsilon_n$  is negative, the  $n$  metal is at a temperature  $T$  which is between  $T_{cn}$  and  $T_c$ . If  $\epsilon_n > 0$ , then  $T < T_{cn} < T_c$ . With this  $\epsilon_n$  value, the value of  $\alpha(T)$  is calculated from Eq. (5). This is repeated for different  $S$  values, and  $H_0/H_{c2}$  vs  $\alpha(T)$  is plotted for  $d_s/\xi$ ,  $d_n/\xi$ , and  $\gamma$  constant. The results for  $\gamma = 1$  and  $d_n/\xi$  equal to 1.0 and 2.0 are shown in Figs. 3 and 4, respectively. The graph for  $d_n/\xi = 1.5$  is shown in Ref. 22 and that for  $d_n/\xi = \infty$  in Ref. 7. It can be seen from Fig. 2 that for negative values of  $(d_s/\xi)^2$  (that is for  $T > T_{cn}$  and certain values of  $S$ )  $\epsilon$  can be double valued. Only solutions which lead to the largest magnetic fields (lowest energy) were plotted.

Sometimes it is more convenient to have a plot of  $H_0/H_{c2}$  vs  $\alpha(T)$  for different  $\gamma$  and  $d_s/\xi$  values,

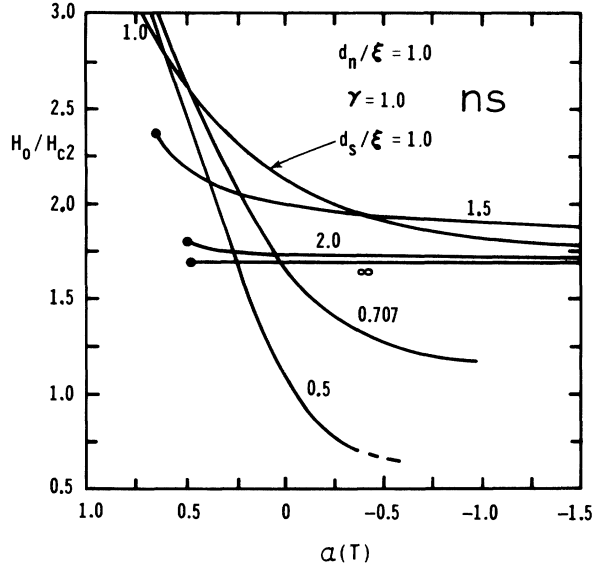


FIG. 3. Nucleation field  $H_0$  of a  $s$ - $n$  double layer, normalized by the *bulk* nucleation field  $H_{c2}$ , for various thicknesses  $d_s$  of the  $s$  layer as a function of the range parameter  $\alpha(T)$  [Eq. (5)] for a strength parameter  $\gamma = 1$  [Eq. (11)]. The thickness of the  $n$  layer  $d_n = \xi$ .  $d_s$  and  $d_n$  are normalized by the *bulk* coherence length  $\xi(T)$  of the  $s$  metal.  $\alpha(T) < 0$  corresponds to temperatures such that  $T_{c,n} < T < T_c$ , and  $\alpha(T) > 0$  to a  $n$  layer in the superconducting state such that  $T < T_{c,n}$ . The solid dots are points where  $S = 0$  [Eq. (6)] at the  $s$ - $n$  interface. The curves shown correspond to  $S > 0$  in Fig. 1.

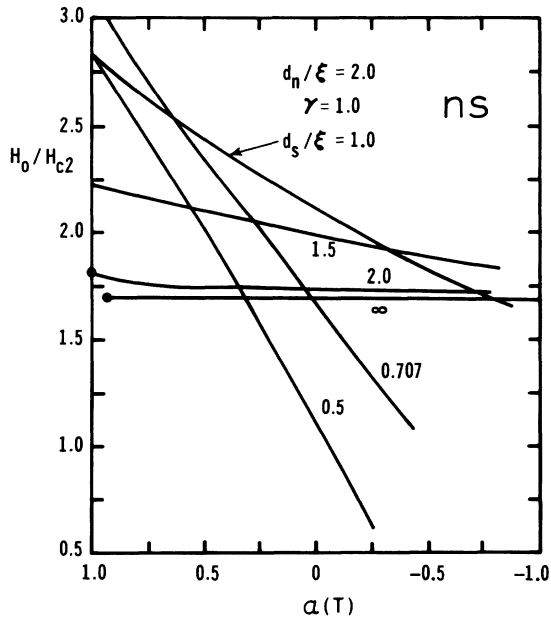


FIG. 4. Similar to Fig. 3 except  $d_n/\xi = 2.0$ .

all for constant  $d_n/\xi$ . Figure 5 shows such a plot when  $d_n/\xi \rightarrow \infty$ . This plot is approximately correct for  $d_n/\xi \geq 2.5$ . From it one can obtain  $\gamma$  values when the  $n$  region is thick. From plots like this one can readily obtain  $\gamma$  values from a measured set of experimental values  $H_0$ ,  $\alpha(T)$ ,  $d_s/\xi$ , and  $d_n/\xi$ .

In order to obtain a value for  $\gamma$  it is necessary to know the ratio of  $m_n \psi_s^2(0^+)/m_s \psi_n^2(0^-)$  in Eq. (11). Essentially, we have to know the boundary condition for the order parameters at the  $sn$  interface. Or if we were able to obtain  $\gamma$  from experiments we could determine the ratio of the order parameters at the  $s$ - $n$  interface.

#### D. Boundary condition

The continuity of the phase current density at the  $s$ - $n$  boundary leads to relations (10) and (11) with  $\gamma$  unspecified. Our solution would be completely specified if  $\gamma$  were known. Thus, a more detailed discussion of the  $\gamma$  parameter is appropriate.

Gor'kov<sup>8</sup> found a relation between the order parameter  $\Psi = \psi e^{i\phi}$  and the pair potential  $\Delta_C$  near  $T_c$  which is

$$\Psi = [\gamma \zeta(3) n \chi(l, T) / 8]^{1/2} (\Delta_C / \pi k T_c), \quad (12)$$

where  $n$  is the total electron density and  $\chi(l, T)$  is a function<sup>8,9</sup> which depends on the mean free path of the electrons when measured just above  $T_c$ . However, such a relation will not be useful for a metal which is intrinsically a normal metal ( $\Delta_{Cn} = 0$  in the bulk) unless we interpret  $\Delta_{Cn}$  near the  $sn$  boundary as an effective pair potential arising from the proximity effect.

When the transition temperatures  $T_{cs}$  and  $T_{cn}$

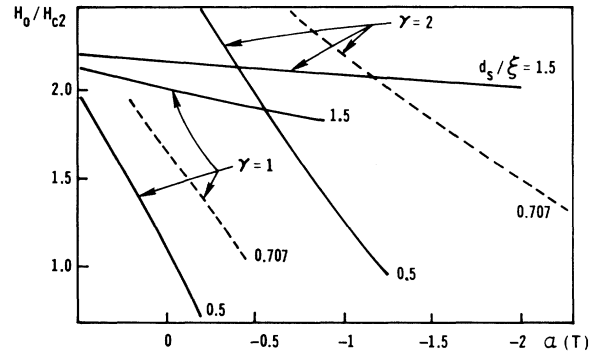


FIG. 5. Theoretical nucleation field  $H_0$  for a  $s$ - $n$  double layer as a function of  $\alpha(T)$  [Eq. (5)] for constant values of  $\gamma$  [Eq. (11)] and constant thickness of the  $s$  layers  $d_s/\xi$  provided the thickness of the  $n$  layers  $d_n > 2\xi$ .  $\xi$  is the *bulk* coherence length of the  $s$  metal and  $H_{c2}$  the *bulk* nucleation field.

are not too far apart, Zaitsev<sup>19</sup> finds that  $\Delta_G$  is continuous for specular and  $m v_F \Delta_G$  for diffuse electron reflections at the  $s$ - $n$  boundary such that

$$\gamma_{sp} = (m_n/m_s)(n_s/n_n)\chi_s/\chi_n \quad (13)$$

and

$$\gamma_{diff} = (m_n v_{Fn}/m_s v_{Fs})^2 \gamma_{sp} . \quad (14)$$

de Gennes<sup>4,5</sup> derived that  $\Delta_G/N(0)V$  is generally continuous, where  $N(0)$  is the local density of states per unit energy and per unit volume at the Fermi level and  $V$  is the effective BCS electron-phonon interaction constant. With this condition one obtains

$$\gamma_{DG} = (N_s(0)V_s/N_n(0)V_n)^2 \gamma_{sp} . \quad (15)$$

We shall investigate below our experimental results with regard to the various  $\gamma$  values (13)–(15).

### III. EXPERIMENTAL TECHNIQUE

Our experiments were performed on Pb-Cu and Pb-Sn double layers which are good proximity systems. Tin was chosen because it was interesting to study the proximity effect of a superconductor on a metal which is a weaker superconductor ( $T_{cn} = 3.8^\circ\text{K}$  for Sn).

Our samples were vapor deposited from heated boats onto glass substrates in a standard bell jar. The vacuum was approximately  $10^{-6}$  Torr. The  $n$  material was evaporated on  $\frac{2}{3}$  of the left-hand side and the  $s$  material on  $\frac{2}{3}$  of the right-hand side of the substrate (Fig. 6). To avoid edge effects the films were scribed under a microscope. The mean free paths  $l$  were determined by the resis-

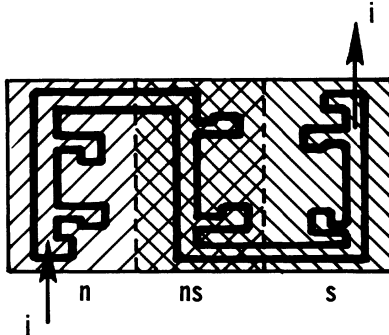


FIG. 6. Sequence of evaporation of the  $n$  and  $s$  materials and sample geometry. The substrate is glass. First the left-hand  $\frac{2}{3}$  of the substrate were coated by the  $n$  material. Then the right-hand  $\frac{2}{3}$  of the substrate were coated with lead. Then the films were scribed. On the left is the test  $n$  film, in the middle the  $s$ - $n$  proximity system and on the right the test  $s$  film. The contacts for the electrical leads are also shown.

tance ratio between room and helium temperatures of the test films in the normal state.

Typical mean free paths at ambient and helium temperatures for Cu, Sn, and Pb were 450, 1600 Å; 110, 1600 Å; and 50, 1500 Å, respectively.

The critical magnetic fields were determined resistively. The current density did not exceed 100 A/cm<sup>2</sup> and did not affect the value of the critical field and critical temperature. The resistive transitions were sharp and the critical magnetic field was determined as the magnetic field corresponding to  $R/R_n = 0.5$ , where  $R_n$  is the resistance in the normal state. The thickness of each layer was monitored with a calibrated quartz crystal oscillator and measured optically within an accuracy of  $\pm 8\%$ .

The samples were mounted in a variable temperature cryostat. Temperatures below 4.2°K were obtained by pumping over the helium bath. Temperatures above 4.2°K were obtained by heating resistors inside the substrate holder. Temperatures were measured with a calibrated cryocal germanium resistor with an accuracy of  $\pm 1\%$ .

### IV. RESULTS AND DISCUSSION

#### A. Determination of $H_{c2}$ , $\xi$ , and $\xi_n$

The value of  $H_{c2}$  used in the normalization of the upper critical magnetic field  $H_0$  was obtained by measuring the parallel nucleation field  $H_{||}$  of the test film. We have used the Saint-James-de Gennes<sup>20,23</sup> curve  $H_{c2}/H_r$  vs  $H_{||}/H_r$  (Fig. 7). The magnetic fields are normalized by the reference field  $H_r = \phi_0/2\pi d_s^2$ , where  $\phi_0 = hc/2e$  is the flux

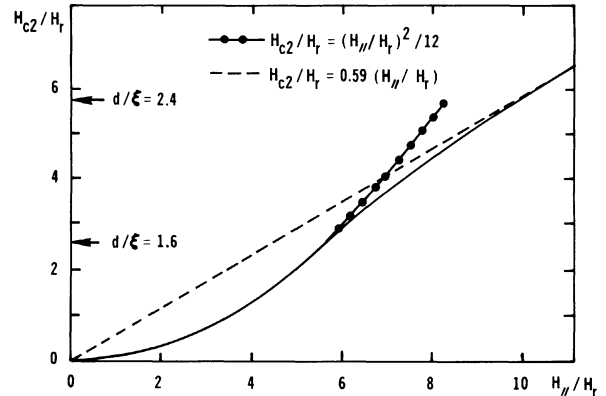


FIG. 7. Parallel nucleation field without proximity effect  $H_{||}(s)$  as a function of the bulk nucleation field  $H_{c2} = \phi_0/2\pi\xi^2$  normalized by the reference field  $H_r = \phi_0/2\pi d^2$ , where  $d$  is the thickness of the superconducting layer. Note that  $H_{c2}/H_r = (d/\xi)^2$ , where  $\xi$  is the coherence length as measured in the  $s$  bulk. The equations shown give good approximations for  $d/\xi < 1.6$  and  $d/\xi > 2.4$ .

quantum. The coherence length of the  $s$  metal is determined from the experimental value of  $H_{c2}$  using the relation  $\xi^2 = \phi_0/2\pi H_{c2}$ .

The coherence length of the normal metal was obtained from<sup>3,6</sup>  $\xi_n^2 = -\xi_T \xi_{PT}/3$  with  $\xi_T = \hbar v_{Fn}/2\pi kT$  and  $\xi_{PT}^{-1} = (3\xi_T)^{-1} + l_n^{-1}$ . For Cu we used  $v_{FCu} = 1.13 \times 10^8$  cm/sec.

For tin,  $|\xi_n| = 0.74(\xi_0 \xi_P)^{1/2}/(t-1)^{1/2}$  for  $t = T/T_{cn} > 1$ , and  $|\xi_n| = 0.74(\xi_0 \xi_P)^{1/2}/(1-t)^{1/2}$  for  $t < 1$  with  $\xi_0 = 2300$  Å ( $v_{FSn} = 0.76 \times 10^8$  cm/sec) and  $\xi_P^{-1} = \xi_0^{-1} + 0.754l^{-1}$ .

### B. Pb-Cu experiments

We discuss here two typical experiments: (a) [ $d_{pb} = 1450$  Å,  $d_{Cu} = 1380$  Å] and (b) [ $d_{pb} = 840$  Å,  $d_{Cu} = 870$  Å]. The nucleation fields  $H_0$  versus temperature for these Pb-Cu sandwiches are shown in Figs. 8 and 9, respectively.

Near the transition temperatures  $T_{csn}$  of the double layers the variation of  $H_0^2$  versus temperature is linear. This is a general result for parallel nucleation fields near the critical temperature.<sup>1</sup>

In experiment (a) (Fig. 8) the variations of  $H_0$  versus temperature are linear at low temperatures and the values of  $H_0$  approach the values of the parallel nucleation field  $H_{||}$  of the lead test film. This indicates that copper does not affect the nucleation process at the free surface of the

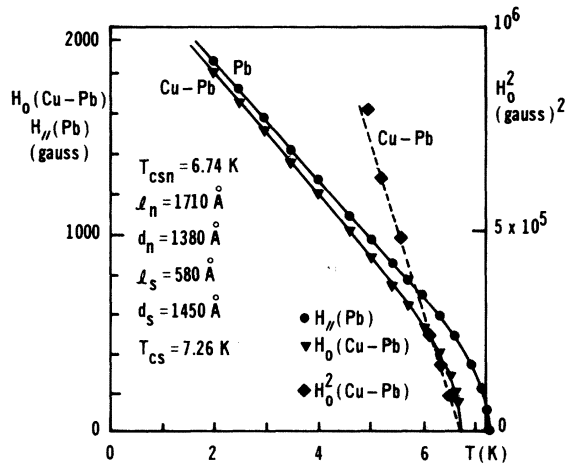


FIG. 8. Experimental results of the parallel nucleation fields  $H_0$  of a Pb-Cu sandwich and that of the test Pb film  $H_{||}$  as a function of temperature  $T$ . Near the transition temperature  $T_{csn}$  the  $H_0^2$  value is a linear function of  $T_{csn} - T$ . At low temperatures the thickness of Pb is large compared to the coherence length  $\xi(T)$  and superconductivity nucleates unimpeded at the free surface of Pb. Therefore the nucleation fields are nearly the same for both specimens at low temperatures and close to  $H_{c3}$ , the surface nucleation field.

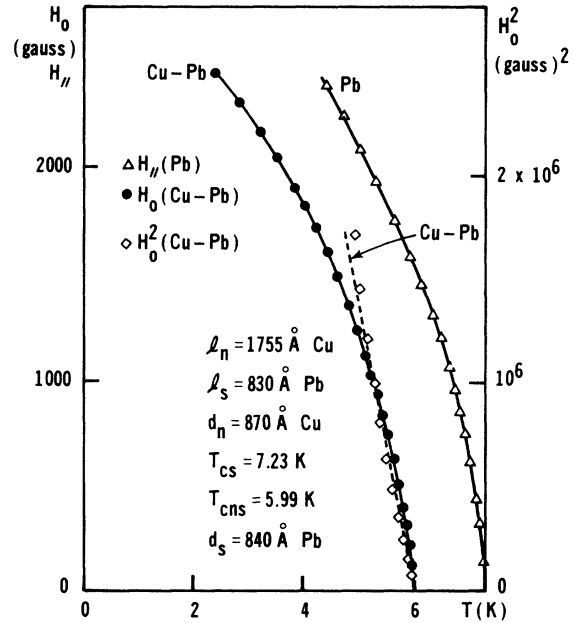


FIG. 9. Experimental results of the parallel nucleation field  $H_0$  of a Pb-Cu sandwich and that of the test Pb film  $H_{||}$  as a function of temperature  $T$  when the thickness of the  $s$  film is small compared to  $\xi(T)$ .  $H_0^2$  is a linear function of  $T_{csn} - T$  near  $T_{csn}$ . Note that  $H_0$  is always appreciably smaller than  $H_{||}$ .

$s$  metal of the  $s-n$  systems. Due to the large thickness of the  $s$  metal compared to the coherence length  $\xi(T)$  the nucleation processes near the surfaces of the  $s$  film are not correlated and the upper critical field is determined by that of the free Pb surface while that near the  $s-n$  interface is suppressed in large magnetic fields. Therefore, the values of  $H_0$  are nearly the same as that of the surface nucleation field  $H_{c3}$ .<sup>23</sup>

In experiment (b), the thickness of the Pb film is small compared to  $\xi(T)$  over the whole range of temperatures. The nucleation process extends over the whole thickness of the  $s$  metal and is influenced by the  $n$  metal. The parallel nucleation field  $H_0$  is lower than  $H_{||}$  of the lead test film even at low temperatures (Fig. 9).

With the data obtained and worked out as explained in Sec. IV A the experimental magnetic field  $H_0(\text{Pb-Cu})$  is plotted as a function of  $d_s/\xi$  in Fig. 10.

The other curve in Fig. 10, which is denoted by "theory," was obtained the following way. With the  $\alpha$  values obtained from  $(\xi/\xi_n)^2$ , and the known  $d_s/\xi$  values, the theoretical  $H_0(s-n)/H_{c2}$  values were obtained from the calculated results as shown, for example, in Figs. 3 and 4. Since the latter plots are for constant  $\gamma$  and  $d_n/\xi$  values, we chose the plot  $\gamma = 1$ ,  $d_n/\xi = \infty$  for the calculated

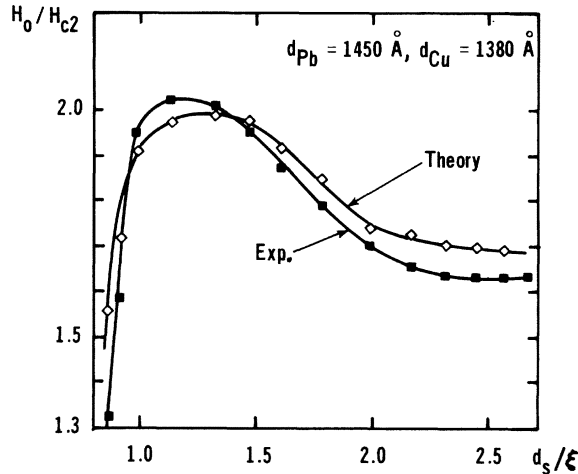


FIG. 10. Experimental (■) and theoretical (◊) results of the parallel nucleation field  $H_0$  normalized by  $H_{c2}$  for the Pb-Cu proximity system whose critical fields are shown in Fig. 8. At low temperatures  $H_0/H_{c2}$  approaches 1.7. As  $d_s/\xi$  decreases ( $T$  increases) the value of  $H_0/H_{c2}$  first increases proportional to  $d_s^{-1}$ , goes through a maximum and then goes to zero at  $T = T_{csn}$ . The theoretical results are for  $\gamma = 1$ . See text for details.

$d_n/\xi$  values larger than 2.5, and the other plots corresponding to the closest experimental values of  $d_n/\xi$ . Plots for  $d_n/\xi = 0.707$  and 0.5 were also available. The interpolated points thus obtained are shown in Fig. 10 for  $\gamma = 1$ . We found that for  $\gamma \approx 1$  we could fit reasonably well all our experimental data for Pb-Cu. We could improve the fit by adjusting the thickness of the  $s$  and/or  $n$  layer within the accuracy of the thickness measurements. The agreement was fairly good considering that there are no other adjustable parameters in the theory, except the value of  $\gamma$  which is directly related to the boundary condition at the  $s$ - $n$  interface. For very small values of  $d_s/\xi$ , that is when  $T \rightarrow T_{csn}$ , there was usually a discrepancy, in that the theoretical curve gave rise to larger  $H_0/H_{c2}$  values than obtained experimentally. For those specimens for which we were able to reach the thick limit  $d_s/\xi \gtrsim 2.5$ , the values of  $H_0/H_{c2}$  reach the limiting value  $H_{c3}/H_{c2} = 1.7$ , indicating that the free surface of the  $s$  layer controls the nucleation field.

For those specimens for which  $d_n/\xi$  was larger than 2 (thick  $n$  limit), we were able to cross check the  $\gamma$  values from a plot  $H_0/H_{c2}$  vs  $\alpha$  with  $d_s/\xi$  and  $\gamma$  constant parameters. It was always found that the value of  $\gamma$  was near unity for the Pb-Cu system over a large range of temperatures and thicknesses of the Pb layers.

Figure 5 shows a plot of  $H_0/H_{c2}$  vs  $\alpha$  [Eq. (5)]

for various constant  $\gamma$  values and constant  $d_s/\xi$  values when  $d_n/\xi \rightarrow \infty$ . The latter condition is satisfied for practical situations when  $d_n/\xi \gtrsim 2.0$ . From such a plot the  $\gamma$  values were obtained from the measured  $H_0/H_{c2}$ ,  $\alpha$ , and  $d_s/\xi$  values when the  $n$  layer was thick. The experimental  $\gamma$  values thus obtained are shown in Fig. 11 by the crosses. From Fig. 11 it is clear that  $\gamma \approx 1$ .

### C. Pb-Sn experiments

Figures 12-14 show the parallel nucleation fields for three of our Pb-Sn specimens as well as those of the Pb and Sn single layers. For a reasonable thick  $n$  layer the transition temperature of the Pb-Sn sandwich decreases as the thickness of the  $s$  layer is decreased. The S shape of the critical field is typical of all the Pb-Sn double layers investigated but not of Pb-Cu sandwiches provided Pb is thin.

The specimen whose critical fields are shown in Fig. 13 was characterized by the following data:  $T_{cs} = 7.26^\circ\text{K}$ ,  $T_{csn} = 6.34^\circ\text{K}$ ,  $T_{cn} = 3.95^\circ\text{K}$ ,  $l_s = 1175 \text{ \AA}$  and  $l_n = 2280 \text{ \AA}$ . The Sn data were analyzed as explained in Sec. IV and the measured field  $H_0(\text{Pb-Sn})$  is plotted as a function of  $d_s/\xi$  in Fig. 15 and is denoted by "experiment." The theoretical curve denoted by "theory" is also shown in Fig. 15 for  $\gamma = 1$ . The general features of these curves with respect to  $d_s/\xi$  are similar to those of the Pb/Cu system (see, e.g., Fig. 10).

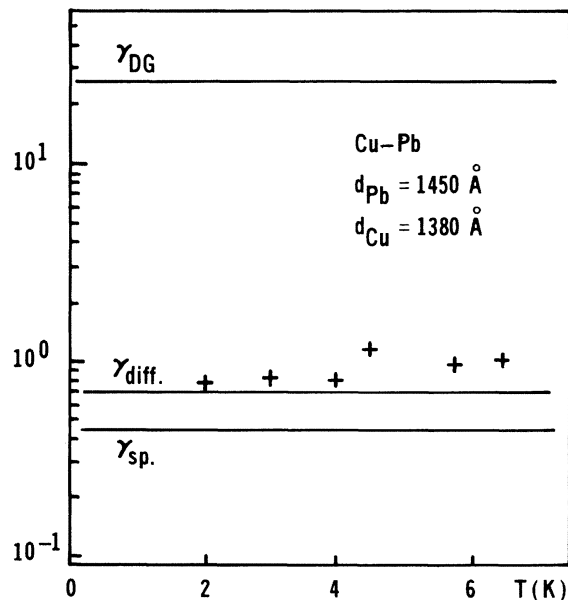


FIG. 11. Comparison of the various theoretical  $\gamma$  values defined by Eqs. (13)-(15) and the experimentally obtained  $\gamma$  for the Pb-Cu specimen as shown in Figs. 8 and 10. The experimental values are indicated by the crosses.

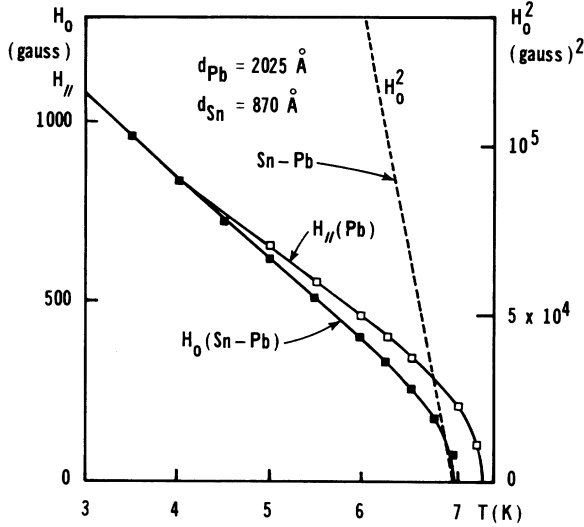


FIG. 12. Experimental results of the parallel nucleation field  $H_0$  of a Pb-Sn sandwich and that of the test Pb and Sn films  $H_{||}$  as a function of temperature. The Pb film is thick compared to  $\xi(T)$  for  $T \lesssim T_{cSn}$ .  $H_0^2$  is a linear function of  $T_{cSn} - T$  near  $T_{cSn}$ . At low temperatures  $H_0 \rightarrow H_{||} \rightarrow H_{c3} \approx 1.7 H_{c2}$  of Pb.

The S-shaped curve of  $H_0(\text{Pb-Sn})$  versus temperature is more striking when the Sn film is thick and the Pb film is thin (compare Figs. 12-14). We propose the following qualitative explanation

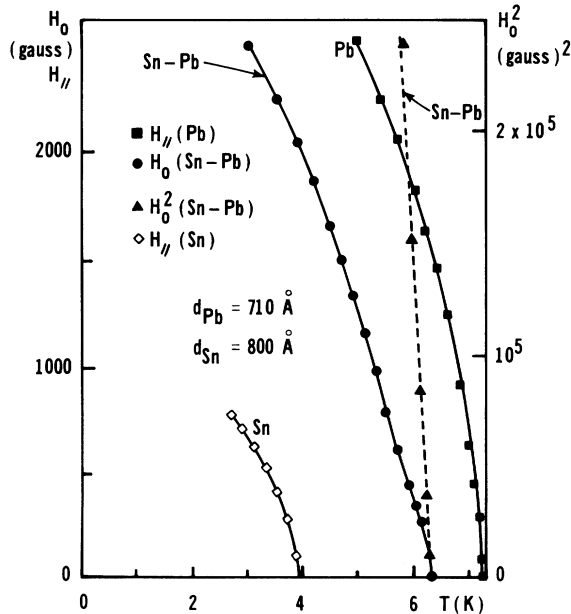


FIG. 13. Similar to Fig. 12 except that the thickness of the Pb film is comparable to  $\xi(T)$ . The critical field curve  $H_0(T)$  of Pb-Sn is S shaped as a function of temperature.

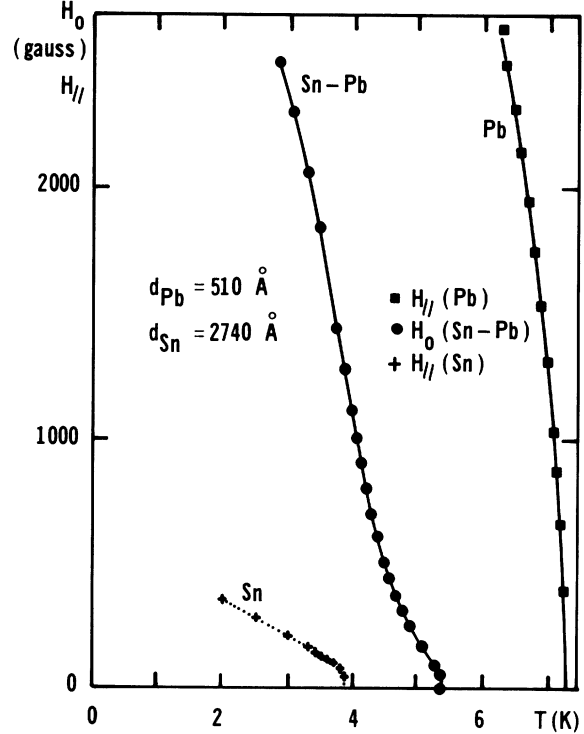


FIG. 14. Similar to Fig. 13 except that the Sn film is thick compared to  $\xi(T)$ . The S-shaped structure of  $H_0(T)$  as a function of  $T$  of the Pb-Sn sandwich is more pronounced than that in Fig. 13.

tion for the S-shaped curves of the Pb-Sn specimens as shown in Figs. 13 and 14. In large magnetic fields the temperature dependence of the magnetic field curve of the Pb-Sn specimens follows parallel to that of the Pb layers similar to that of the Pb-Cu specimens which, however, follow the Pb layers for all measured fields, even for low fields. In large magnetic fields superconductivity is quenched in Sn and it behaves therefore, intrinsically like a normal metal with an extrapolation length  $|\xi_n| \propto T^{-1/2}$  in the dirty limit. In the other extreme, mainly the low-field limit, the temperature dependence of the Pb-Sn critical field is parallel to that of the Sn layer and in this limit as  $H_0 \rightarrow 0$  the extrapolation length  $|\xi_n|$  must be controlled by  $(T - T_{c_n})^{-1/2}$ . Thus it becomes apparent that  $|\xi_n|$  for Sn should also be magnetic field dependent. Our experiments can be qualitatively described for Sn by using  $|\xi_n| \propto [T - T_{c_n}(H)]^{-1/2}$ , where  $T_{c_n}(H) \rightarrow 0$  in the high field and  $T_{c_n}(H) \rightarrow T_{c_n}$  in the low-field limit.

## V. CONCLUSION

The boundary conditions which we used in our calculations apply to both the Pb-Cu and the Pb-



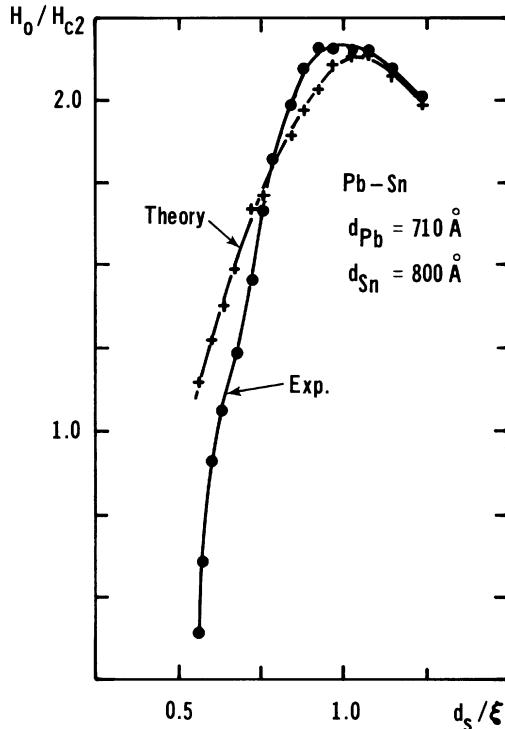


FIG. 15. Experimental (●) and theoretical (+) results of the parallel nucleation field  $H_0$  normalized by  $H_{c2}$  for the Pb-Sn proximity system whose critical fields are shown in Fig. 13. The theoretical results are for  $\gamma=1$ .

Sn systems with  $\gamma=1$ . This means that  $|\Psi|$  or  $|\Delta_G|$  is approximately continuous across the  $s$ - $n$  boundary. Within the accuracy of our interpolated numerical and experimental results we cannot say whether the specular or diffused electron reflection condition at the  $s$ - $n$  interface applies, but the diffused reflection condition appears to be the more likely case.

It is the conclusion of the present investigation that this boundary condition applies at the  $s$ - $n$  interface regardless of the thickness  $d_s$  and  $d_n$  of the  $s$  and  $n$  layers over a wide range of temperatures.

This conclusion is reached regardless of whether or not the  $n$  metal is intrinsically a superconductor, such as Sn, or a normal metal, such as Cu, which may or may not become a superconductor very close to absolute zero. As can be seen from Figs. 10, 11, and 15 the  $\gamma$  value is near unity and temperature independent. This conclusion is simi-

lar to that of Ref. 20 for  $n$ - $s$ - $n$  layers but different from that of Todd *et al.*<sup>18</sup> for  $s$ - $n$  layers for the thin  $s$  limit, probably because of their comparison of their experimental results with a theory that is limited to  $d_n=\infty$  and the way they determined the bulk nucleation field  $H_{c2}$ .

The continuity of  $\Delta_G$  is a natural consequence of a comparison of theory with the experimental results. However, we would like to point out that  $\Delta_{Gn}$  is an effective pair potential near the  $s$ - $n$  boundary, induced by the proximity effect, and not that of the  $n$  metal far away from the  $s$ - $n$  boundary (in the bulk). In order to be consistent with the de Gennes boundary condition<sup>4,5</sup> we must relate  $\Delta_{Gn}$  to the pair amplitude ("condensation amplitude")  $F_n = \langle \psi \dagger \psi \dagger \rangle$  by

$$\Delta_{Gn} = V_s F_n. \quad (16)$$

Then the continuity of  $\Delta$  at the  $s$ - $n$  boundary is the same as the continuity of  $F$ .

To understand this result we suggest the following interpretation: Pairs diffuse or tunnel from the superconductor into the normal metal while normallike electrons move in the opposite direction such that in the time average charge neutrality will be conserved. Since pairs cannot break up instantaneously into single electrons in the  $n$  metal and single electrons cannot pair instantaneously in the  $s$  metal, the pairs will carry with them into the  $n$  metal the memory of the  $[N(0)V]_s$  interaction which will be retained for a certain time  $\tau$  regardless of what the intrinsic bulk  $[N(0)V]_n$  interaction of the new host metal is, even when the latter is zero. Thus in the time average a reduced number of pairs will live in the  $n$  metal paired by the  $[N(0)V]_s$  interaction and the exact number density depends on the rate with which they are supplied to the  $n$  region by the  $s$  region and the rate with which they decay, thus giving rise in the time average to an effective decay length  $|\xi_n|$  in the  $n$  region so that  $\tau = |\xi_n|/v_F$ .

#### ACKNOWLEDGMENTS

We thank G. Deutscher for discussions regarding boundary conditions. One of us (H.J.F.) acknowledges discussion with K. H. Bennemann regarding the proximity effect. We are obliged to A. G. Presson and R. S. Poulsen for their help with the numerical solutions.

\*Supported in part by NSF Grant No. ENG73-08279 A01 and a faculty research grant from the University of California, Davis.

<sup>1</sup>Orsay Group on Superconductivity, in *Quantum Fluids*, edited by D. F. Brewer (North-Holland, Amsterdam,

1966), pp. 26-67.

<sup>2</sup>G. Deutscher, *J. Phys. Chem. Solids* **28**, 741 (1967).

<sup>3</sup>J. P. Hurault, thesis (University of Paris, Orsay, 1968) (unpublished); and *Phys. Lett.* **20**, 587 (1966).

<sup>4</sup>P. G. de Gennes, *Rev. Mod. Phys.* **36**, 225 (1964).

- <sup>5</sup>G. Deutscher and P. G. de Gennes, in *Superconductivity*, edited by R. D. Parks (Marcel Dekker, New York, 1969), p. 1005.
- <sup>6</sup>H. J. Fink and A. G. Presson, *Phys. Rev. B* 1, 221 (1970).
- <sup>7</sup>H. J. Fink and P. Martinoli, *J. Low Temp. Phys.* 4, 305 (1971).
- <sup>8</sup>L. P. Gor'kov, *Zh. Eksp. Teor. Fiz.* 37, 1407 (1959) [*Sov. Phys.-JETP* 10, 998 (1960)].
- <sup>9</sup>C. F. Hempstead and Y. B. Kim, *Phys. Rev. Lett.* 12, 145 (1964).
- <sup>10</sup>S. Gygax and R. H. Kroppschot, *Phys. Lett.* 9, 91 (1964).
- <sup>11</sup>L. J. Barnes and H. J. Fink, *Phys. Lett.* 20, 583 (1966).
- <sup>12</sup>L. J. Barnes and H. J. Fink, *Phys. Rev.* 149, 186 (1966).
- <sup>13</sup>G. Fischer and R. Klein, *Proceedings of the Tenth International Conference on Low-Temperature Physics, Moscow, 1966*, edited by M. P. Malkov (VINITI, Moscow, 1967), p. 197; and *Phys. Lett.* 23, 311 (1966).
- <sup>14</sup>G. Fischer and R. Klein, *Phys. Kondens. Mater.* 7, 12 (1968).
- <sup>15</sup>P. Martinoli, *Solid State Commun.* 9, 2177 (1971).
- <sup>16</sup>P. Martinoli, *Phys. Kondens. Mater.* 16, 53 (1973).
- <sup>17</sup>R. J. Todd, J. T. Chen, and Y. W. Kim, *Phys. Rev. B* 5, 2518 (1972).
- <sup>18</sup>R. J. Todd, J. T. Chen, and Y. W. Kim, *Phys. Rev. B* 7, 150 (1973).
- <sup>19</sup>R. O. Zaitsev, *Zh. Eksp. Teor. Fiz.* 50, 1055 (1966) [*Sov. Phys.-JETP* 23, 702 (1966)].
- <sup>20</sup>H. J. Fink, *J. Low Temp. Phys.* 16, 387 (1974).
- <sup>21</sup>M. C. Jain and D. R. Tilley, *J. Low Temp. Phys.* 9, 449 (1972).
- <sup>22</sup>H. J. Fink, M. Sheikholeslam, M. R. Esfandiari, A. Gilbert, J. P. Romagnan, J. P. Laheurte, and J. C. Noiray, *Fourteenth International Conference on Low-Temperature Physics* (North-Holland, Amsterdam, 1975), Vol. 2, pp. 191-194.
- <sup>23</sup>D. Saint-James and P. G. de Gennes, *Phys. Lett.* 7, 306 (1963).